Dyes and Pigments 196 (2021) 109784

Contents lists available at ScienceDirect

Dyes and Pigments

journal homepage: www.elsevier.com/locate/dyepig

Synthesis and characterization of aryl-substituted BODIPY dyes displaying distinct solvatochromic singlet oxygen photosensitization efficiencies

Raquel C.R. Gonçalves [a], João Pina [b,*], Susana P.G. Costa [a], M. Manuela M. Raposo [a,**]

[a] Centre of Chemistry, University of Minho, Campus de Gualtar, 4710-057, Braga, Portugal
[b] University of Coimbra, Coimbra Chemistry Centre, Department of Chemistry, Rua Larga, 3004-535, Coimbra, Portugal

ARTICLE INFO

Keywords:
BODIPY
Photosensitizers
Singlet oxygen
Intramolecular charge transfer

ABSTRACT

Three BODIPY derivatives substituted at *meso* position by aryl (phenyl or *N,N*-dimethylaminonaphthyl) groups and functionalized at position 2 with electron-withdrawing formyl or electron deficient benzimidazole heterocycle were synthesized and completely characterized by the usual spectroscopic techniques. A comprehensive photophysical study showed a remarkable enhancement of the singlet oxygen sensitization quantum yield for *meso*-substituted dimethylaminonaphthyl BODIPY with the decrease of the dielectric constant of the solvent (0.02–0.04 for dimethylsulfoxide *vs.* 0.84 in toluene). In toluene the triplet state formation for the aminonaphthyl substituted BODIPY's was found to be mediated by the intramolecular charge transfer state (ICT), whereas in polar solvents triplet state formation is hindered by fast recombination of the ICT state. Pump-probe transient absorption spectroscopy was used to characterize the photoinduced dynamics of the BODIPY derivatives from the femtosecond to the nanosecond time scale.

1. Introduction

Photodynamic therapy (PDT) represents a non-invasive alternative approach for cancer treatment and involves the combination of three main elements: a photosensitizer (PS), a source of light with an appropriate wavelength and molecular oxygen. Photosensitizers are a group of molecules activated by photons in order to generate reactive oxygen species (ROS) responsible for oxidation of proteins, lipid peroxidation, enzyme inhibition and DNA damage, which will trigger apoptotic pathways that lead to cell death. Upon light irradiation, photosensitizer goes through activation from the singlet ground state to the singlet excited state and rapidly decays, *via* intersystem crossing (ISC), to triplet excited state. PS triplet excited state transfers its energy to molecular oxygen to form singlet oxygen $^1O_2$ [1,2]. Thus, monitoring singlet oxygen generation, commonly represented as $^1O_2$ quantum yield (ϕ_Δ), is extremely important to evaluate the efficiency of new photodynamic therapy agents.

A number of molecular structures have been widely studied for PDT, such as tetrapyrrole derivatives, synthetic dye classes such as phenothiazinium, squaraine, transition metal complexes and natural products including hypericin, riboflavin and curcumin. However, traditional photosensitizers display a flat structure which tends to interact with adjacent molecules through π–π stacking. This enhances the excited state internal conversion deactivation channel, decreasing intersystem crossing to form the PS triplet excited state and concomitanly reducing their $^1O_2$ sensitization quantum yield [3–7].

During the past years several approaches have been attempted to fine-tune BODIPY framework towards suitable PDT agents [8–10]. BODIPY dyes are unique fluorophores displaying impressive spectroscopic and photophysical property changes upon substitution of functional groups on the main core structure [11–13]. Substitution of the BODIPY backbone with electron-donating groups at position 8 (*meso*-position) originates a blue shifted fluorescence emission while substitution at positions 3 and 5 generally originates higher bathochromic shift than positions 2 and 6 [14]. Orte et al. reported the effect of substituent side groups like phenyl, styryl or phenylethynyl at the 2-, 3- or 8-position of BODIPY [15]. It was shown that substitution at 3-position originated BODIPYs with sharp absorption bands and high fluorescence quantum yields, while substitution at the 2-position yielded BODIPYs with large Stokes shifts and broad bands. Substitution at the *meso*-position produced dyes with features like the 3-substituted ones, except for *meso*-phenyl BODIPY. Previous studies showed that by

* Corresponding author.
** Corresponding author.
E-mail addresses: jpina@qui.uc.pt (J. Pina), mfox@quimica.uminho.pt (M.M.M. Raposo).

https://doi.org/10.1016/j.dyepig.2021.109784
Received 27 May 2021; Received in revised form 1 August 2021; Accepted 1 September 2021
Available online 3 September 2021

attaching electron-donor groups at *meso*-phenyl and *meso*-naphthyl moieties induced photoinduced electron or charge transfer (PET or PCT), which enables BODIPYs to generate T_1 state via charge recombination [16]. However, pristine *meso*-phenyl or naphthyl substitution showed no improvement in generating T_1 state and singlet oxygen for BODIPYs, which was attributed to the low electron donating ability of phenyl or naphthyl groups [16]. Non-halogenated BODIPYs are well known for their high fluorescence quantum yields, however, recently BODIPY derivatives displaying high triplet state formation and singlet oxygen photosensitization have been described [17], broadening the application of these chromophores to photodynamic therapy and theranostics. The excited triplet state formation and singlet oxygen sensitization efficiency of BODIPY derivatives is influenced by the electron donor/acceptor strength of the substituent moiety, solvent polarity and the substituent position [16,18,19].

The present work is focused on the influence of the electron donor/withdrawing substituents at *meso* and 2-positions of the BODIPY core and solvent polarity on the singlet oxygen photosensitization efficiency of BODIPY, as well on their photophysical properties.

2. Experimental

All reagents were purchased from Sigma-Aldrich, Acros and Fluka and used as received. TLC analyses were carried out on 0.25 mm thick pre-coated silica plates (Merck Fertigplatten Kieselgel 60F254) and spots were visualized under UV light. Chromatography on silica gel was carried out on Merck Kieselgel (230–400 mesh).

NMR spectra were obtained on a Bruker Avance III 400 at an operating frequency of 400 MHz for ^{1}H and 100.6 MHz for ^{13}C, at 25 °C using the solvent peak as an internal reference. All chemical shifts are given in ppm using δ_H $Me_4Si = 0$ ppm as reference. Assignments were supported by spin decoupling-double resonance and bidimensional heteronuclear techniques. Low and high resolution mass spectra were obtained at "C.A. C.T.I.—*Unidad de Espectrometria de Masas*" at the University of Vigo, Spain. The synthesis of BODIPY precursors **3i** and **3ii** is given in the Supporting Information. BODIPY precursors **3i-ii** and BODIPY derivative **3** have been reported elsewhere [18,20].

2.1. Synthesis of naphthyl-substituted BODIPY derivative *1*

2,4-Dimethylpyrrole (2.0 mmol) and 4-dimethylamino-1-naphthaldehyde (1.0 mmol) were dissolved in dry dichloromethane (100 mL). One drop of trifluoroacetic acid was added and the mixture was allowed to stir for 50 min at room temperature. A solution of 2,3-dichloro-5,6-dicyano-1,4-benzoquinone (DDQ) (2.0 mmol) in dry dichloromethane (100 mL) was added to the mixture. Stirring was continued for another 50 min and then triethylamine (16.3 mmol) was added. After stirring for 15 min, $BF_3{\cdot}OEt_2$ (27.6 mmol) was added and further stirred for 30 min. The solvent was evaporated under reduced pressure and the crude residue was purified by dry flash chromatography (petroleum ether/ethyl acetate, 4:1). The product was obtained as a dark red solid (0.146 g, 35%).

^{1}H NMR (400 MHz, $CDCl_3$): $\delta = 1.09$ (s, 6H, CH_3-1 and CH_3-7), 2.58 (s, 6H, CH_3-3 and CH_3-5), 3.05 (s, 6H, $N(CH_3)_2$), 5.94 (s, 2H, H-2 and H-6), 7.25 (d, $J = 7.6$ Hz, 1H, H-2′), 7.30 (d, $J = 7.6$ Hz, 1H, H-3′), 7.44 (dt, $J = 1.2$ and 7.2 Hz, 1H, H-7′), 7.54 (dt, $J = 1.2$ and 7.4 Hz, H-6′), 7.77 (d, $J = 8.4$ Hz, 1H, H-5′), 8.31 (d, $J = 8.4$ Hz, 1H, H-8') ppm.

^{13}C NMR (100.6 MHz, $CDCl_3$): $\delta = 13.89$ (CH_3-1 and CH_3-7), 14.60 (CH_3-3 and CH_3-5), 45.53 ($N(CH_3)_2$), 114.08 (C2′), 121.07 (C2 and C6), 123.88 (C8′), 125.55 (C5′), 125.83 (C3′), 126.16 (C6′), 127.18 (C7′), 128.04 (C4′), 132.19 (C7a and C8a), 132.95 (C4′a and C8′a), 140.36 (C8), 143.01 (C1 and C7), 150.25 (C1′), 155.43 (C3 and C5) ppm.

MS (ESI) *m/z* (%): 419 ($[M + 2]^{+\bullet}$, 27), 418 ($[M + 1]^{+\bullet}$, 100), 417 ($[M]^{+\bullet}$, 40), 291 (4), 102 (5); HRMS (ESI) *m/z*: $[M + 1]^{+\bullet}$ calcd for $C_{25}H_{27}BF_2N_3$, 418.2261; found 418.2269.

2.2. Synthesis of naphtyl-substituted BODIPY derivative *2*

A mixture of *N,N*-dimethylformamide (23 mmol) and $POCl_3$ (18.2 mmol) was stirred for 5 min at 0 °C under N_2 atmosphere. The mixture was allowed to reach room temperature and stirred for additional 30 min. Compound **1** (0.127 mmol) dissolved in dichloroethane (7 mL) was added dropwise while stirring. The reaction mixture was heated for 2 h at 50 °C. After cooling, the solution was poured slowly into 40 mL of saturated sodium bicarbonate solution at 0 °C and stirred for 30 min at room temperature. Ethyl acetate (5 mL) was added to the reaction mixture and the resulting organic layer separated and washed with water (2 × 50 mL). The organic layer was dried with anhydrous $MgSO_4$ and filtered. After evaporation of the solvent to dryness, the crude residue was purified by a silica gel chromatography column, using dichloromethane as eluent. The product was obtained as a dark red solid (0.126 g, 57%).

^{1}H NMR (400 MHz, $CDCl_3$): $\delta = 1.12$ (s, 3H, CH_3-7), 1.37 (s, 3H, CH_3-1), 2.64 (s, 3H, CH_3-5), 2.84 (s, 3H, CH_3-3), 3.13 (s, 6H, $N(CH_3)_2$), 6.11 (s, 1H, H-6), 7.33 (m, 2H, H-2′ and H-3′), 7.48 (t, $J = 7.6$ Hz, 1H, H-7′), 7.62 (t, $J = 7.6$ Hz, H-6′), 7.72 (d, $J = 8.4$ Hz, 1H, H-5′), 8.31 (s, 1H, H-8'), 9.94 (s, 1H, CHO) ppm.

^{13}C NMR (100.6 MHz, $CDCl_3$): $\delta = 10.99$ (CH_3-1), 13.03 (CH_3-3), 14.40 (CH_3-7), 15.09 (CH_3-5), 45.69 ($N(CH_3)_2$), 124.01 (C6), 125.21 (C5′), 124.19 (C8'), 125.60 (C2′ and C3′), 126.19 (C2), 127.03 (C8a), 127.45 (C6′), 127.90 (C7′), 130.26 (C4′), 132.75 (C4′a and C8′a), 134.79 (C7a), 141.80 (C8), 142.51 (C1), 147.01 (C7), 147.19 (C1′), 156.58 (C3), 161.91 (C5), 185.87 (CHO) ppm.

MS (ESI) *m/z* (%): 447 ($[M + 2]^{+\bullet}$, 29), 446 ($[M + 1]^{+\bullet}$, 100), 445 ($[M]^{+\bullet}$, 28), 201 (1); HRMS (ESI) *m/z*: $[M + 1]^{+\bullet}$ calcd for $C_{26}H_{27}BF_2N_3O$, 446.2210; found 446.2208.

2.3. Synthesis of phenyl-substituted BODIPY derivative *3*

Formyl-BODIPY precursor **3ii** [16] (0.07 mmol), ethanol (10 mL) and $NaHSO_3$ (0.15 mmol) were added in a round bottomed flask and stirred at room temperature for 4 h. Then, dry dimethylformamide (5 mL) and *o*-phenylenediamine (0.11 mmol) were added and the reaction solution was heated and stirred for 2 h at 80 °C. After cooling to room temperature, ethyl acetate was added (10 mL) and the mixture was washed with water (3 × 10 mL). The organic phase was dried with anhydrous $MgSO_4$ and the solvent was evaporated to dryness. The crude was purified by silica gel chromatography column using petroleum ether/ethyl acetate (4:1) as eluent and the product was obtained as a red solid (0.039 g, 77%).

^{1}H NMR (400 MHz, $CDCl_3$): $\delta = 1.35$ (s, 3H, CH_3-7), 1.47 (s, 3H, CH_3-1), 2.59 (s, 3H, CH_3-5), 2.67 (s, 3H, CH_3-3), 6.10 (s, 1H, H-6), 7.06–7.07 (m, 2H, H-2′ and H-6′), 7.22–7.24 (m, 2H, H-5″ and H-6″), 7.37–7.40 (m, 3H, H-3′, H-4′ and H-5′), 7.57–7.59 (m, 2H, H-4″ and H-7″) ppm.

^{13}C NMR (100.6 MHz, $CDCl_3$): $\delta = 12.82$ (CH_3-1), 13.45 (CH_3-3), 14.61 (CH_3-7), 14.88 (CH_3-5), 114.56 (C7″ and C4″), 118.80 (C2), 123.13 (C6), 123.60 (C5″ and C6″), 127.60 (C2′ and C6′), 129.27 (C3′, C4′ and C5′), 130.33 (C8a), 133.14 (C7), 134.11 (C1′), 136.12 (C3″a and C7″a), 140.14 (C1), 142.94 (C8), 145.68 (C2″), 146.27 (C7a), 152.45 (C3), 159.71 (C5) ppm.

2.3.1. Photophysical studies

The solvents used were of spectroscopic grade and used as received. Absorption and fluorescence spectra were recorded on a Cary 5000 UV–Vis–NIR and Horiba-Jobin-Ivon Fluorolog 322 spectrometers respectively. All the fluorescence emission spectra were corrected for the wavelength response of the system. Room temperature fluorescence quantum yields were obtained by the comparative method using rubrene in chloroform, $\phi_F = 0.54$, as reference compound [21]. Fluorescence decays were measured with excitation at 460 nm using a home-built time correlated single photon counting, TCSPC, apparatus described elsewhere [22]. Deconvolution of the fluorescence decay

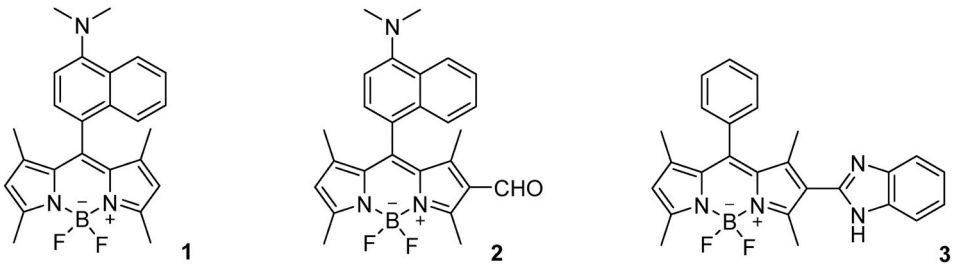

Fig. 1. Structures of the investigated compounds. (**1**–**3**).

curves was performed using the modulating function method, as implemented by G. Striker in the SAND program, as previously reported in the literature [23].

The ground state molecular geometry was optimized on isolated entities in a vacuum without conformation restrictions using the density functional theory (DFT) by Gaussian 09 program [24] at PBE1PBE/6-311g(d,p) level [25]. Frequency analysis for each compound were also computed and did not yield any imaginary frequencies, indicating that the structure of each molecule corresponds to at least a local minimum on the potential energy surface. The frontier orbitals of the molecules based on the optimized ground state geometries were calculated (using the same functional and basis set as those in the previously calculations) and plotted using Gaussview 6.0.

Time resolved ultrafast transient absorption measurements were collected in a broadband HELIOS spectrometer from Ultrafast Systems, equipped with an amplified femtosecond Spectra-Physics Solstice-100F laser (1 kHz repetition rate) coupled with a Spectra-Physics TOPAS Prime F optical parametric amplifier (195–22 000 nm) for pulse pump generation [26]. The transient absorption data was obtained with excitation at 515 and 540 nm and probed in the 350–750 nm range. The measurements in solution were obtained in a 2 mm quartz cuvette, with absorptions ≈0.1 at the pump excitation wavelength. To avoid photodegradation, the solutions were kept in movement using a motorized translating sample holder. The spectral chirp correction and the global analysis (principal component analysis implemented after single value decomposition) of the time resolved data was performed using Surface Xplorer PRO program from Ultrafast Systems.

The experimental setup used to obtain the triplet-triplet absorption spectra and lifetimes consisted of (i) an LKS.60 Laser Flash Photolysis Spectrometer from Applied Photophysics, elsewhere described [22], pumped with the third harmonic (355 nm) of a Nd:YAG Quanta-Ray Spectra Physics laser; or a (ii) nanosecond-millisecond broadband (350–1600 nm) pump-probe Transient Absorption EOS-Fire spectrometer from Ultrafast Systems, which shares the same excitation source as the femtosecond pump-probe spectrometer described above. In this case the transient absorption data was collected with excitation at 480 nm or 500 nm and probed in the 350–800 nm range. Low laser energy was used to avoid multiphoton and triplet-triplet annihilation effects. The solutions used to collect the transient singlet-triplet difference absorption spectra were bubbled with nitrogen for at least 20 min. In general, the obtained transient absorption signals were assigned to the triplet state of the BODIPY derivatives since first-order kinetics were found and strong quenching was observed in the presence of oxygen.

Room-temperature singlet oxygen phosphorescence was detected at 1276 nm with a Hamamatsu R5509-42 photomultiplier cooled to 193 K in a liquid nitrogen chamber (Products for Research model PC176TSCE-005) following laser excitation at 355 nm of aerated solutions of the samples in an adapted Applied Photophysics flash kinetic spectrometer pumped with the Nd:YAG laser described above [22]. The modification of the spectrometer involved the interposition of a 600-line diffraction grating instead of the standard spectrometer, to extend spectral response to the infrared. In addition to avoid the overlap of the fluorescence emission second harmonic signal with the sensitized singlet oxygen phosphorescence emission at 1276 nm a Newport longpass dielectric filter with 1000 nm cut-on (reference 10LWF-1000-B) was used. The sample solutions were optically matched at the excitation wavelength (absorbances less than 0.3) with those of the reference compound Phenalenone, $\phi_\Delta = 0.93$ in toluene solution and $\phi_\Delta = 0.98$ in the polar solvents THF and DMSO [27–31]. The singlet oxygen sensitization quantum yield values (ϕ_Δ) were determined by plotting the initial emission intensity (determined by fitting the decays with a single exponential law in which the pre-exponential value translates the intensity a time zero) of optically matched solutions as a function of the laser energy and comparing the slope with that obtained upon sensitization with the reference compound, see Equation (1):

$$\phi_\Delta^{cp} = \frac{slope^{cp}}{slope^{ref}} \cdot \phi_\Delta^{ref} \quad (1)$$

with ϕ_Δ^{ref} the singlet oxygen formation quantum yield of the reference compound.

Ideally, the same absorbance at the excitation wavelength and mainly the same solvent should be used for the reference and for the photosensitizer under study. However, in cases where the absorbance of the reference and samples compound are not matched at the excitation wavelength and different solvents are used for the photosensitizers and reference compound additional corrections can be introduced in the previous equation.

$$\phi_\Delta^{cp} = \frac{slope^{cp}}{slope^{ref}} \cdot \frac{OD_{ref}}{OD_{cp}} \cdot \frac{n_{cp}^2}{n_{ref}^2} \cdot \phi_\Delta^{ref} \quad (2)$$

where n_x is the refractive index of the solvents in which the compounds and the reference were respectively dissolved and OD_x the optical density of the reference (ref) and compound (cp) at the excitation wavelength. Although in the present work the same solvents were used for the BODIPY derivatives and the reference phenalenone, we would like to highlight that by using the slope of the plot of the phosphorescence signal of singlet oxygen as a function of laser intensity in the ϕ_Δ determination, the dependence of the phosphorescence signal intensity on the singlet oxygen lifetime and oxygen concentration (solvent dependent properties) can be considered negligible, thus no additional corrections are needed in equation (2).

3. Results and discussion

The structures of the investigated compounds are depicted in Fig. 1. These comprise the tetramethyl-BODIPY derivatives **1**–**2** functionalized with an electron-donating *N,N*-dimethylaminonaphthyl group at *meso* (8-position), and a formyl electron-withdrawing group at 2-position, and BODIPY derivative **3** bearing a phenyl group at *meso* position, and a benzimidazole heterocycle at position 2 of the BODIPY core.

The *meso*-substituted BODIPY derivative **1** was obtained by following the well-established Lindsey's method [32]. The synthesis involved the condensation between the aryl aldehyde and 2 equiv. of 2,4-dimethylpyrrole, followed by oxidation with 2,3-dichloro-5,6-dicyano-1,4-benzoquinone (DDQ) and amine-mediated boron chelation to afford the

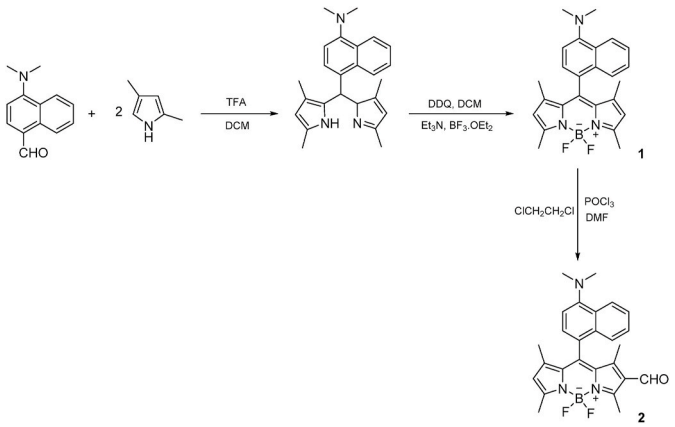

Scheme 1. Synthesis of naphthyl-substituted BODIPY derivatives **1** and **2**.

symmetrical *meso*-substituted *N,N*-dimethylaminonaphthyl-BODIPY. The formylated BODIPY derivative **2** was synthesized through Vilsmeier-Hack reaction by treating compound **1** with Vilsmeier reagent prepared from $POCl_3$ and DMF (Scheme 1). BODIPY precursors **3i** and **ii** were prepared according to procedures described previously (Scheme S1) [20]. The benzimidazole containing BODIPY derivative **3** was prepared through the condensation reaction between *o*-phenylenediamine and formyl-BODIPY precursor **3ii** in the presence of $NaHSO_3$ as activating agent of the diamine (Scheme 2). Compound **3** has been already synthesized and reported by other research group through a different synthetic methodology aiming its application as "off-on" fluorescent pH sensor [18]. Identification of the three BODIPY derivatives **1–3** was performed through ^{1}H and ^{13}C NMR spectroscopy and mass spectrometry. The results were consistent with the predicted structures, as shown in the experimental section.

3.1. Photophysical properties

The absorption and fluorescence emission spectra of the BODIPY derivatives in solvents of different polarity solution are presented in Fig. 2. The absorption spectra show the characteristic absorption features of the BODIPY chromophore with the strong absorption band with maximum at ~495–515 nm and emission maxima at ~515–570 nm [11]. The fluorescence emission spectra of the investigated BODIPY's are strongly solvent dependent. The emission spectra of the amino-naphthyl derivatives in toluene in addition to the characteristic BODIPY emission presents an additional broad and structureless red-shifted emission band (see Fig. 2), that, has described elsewhere is promoted by the presence of the amino group and attributed to intramolecular charge transfer [16]. Noteworthy is that, in polar solvents, the ICT band is not observed due to fast recombination of the ICT state.

For BODIPY **3** although no additional red-shifted emission band was observed, the high Stokes shift (Δ_{SS}) values found for the investigated solvents, together with their concomitant increase, with the solvent dielectric constant values ($\Delta_{SS} = 1874\ cm^{-1}$ in toluene, $\varepsilon_{THF} = 2.379$, $\Delta_{SS} = 2056\ cm^{-1}$ in THF, $\varepsilon_{THF} = 7.58$, and $\Delta_{SS} = 2353\ cm^{-1}$ in DMSO, $\varepsilon_{DMSO} = 46.7$)[21], see Fig. 2, points to the occurrence of charge transfer. This is in agreement with previously reported DFT theoretical calculations which demonstrated that photoinduced electron transfer partly occurs between BODIPY and the benzimidazole moiety [18].

The fluorescence quantum yields (ϕ_F) obtained in polar solvents were found to be in the 0.004–0.007 range for BODIPY **1** and **2,** in agreement to what was previously reported [18], while for **3** values of $\phi_F = 0.33$ and 0.14 in THF and DMSO solutions were respectively obtained, see Table 1. Going to the non-polar solvent toluene, in general, the ϕ_F values are significantly higher than those found in polar solvents, $\phi_F = 0.058$ (**1**), 0.047 (**2**) and 0.56 (**3**), see Table 1.

Comparison with the 1,3,5,7-tetramethyl-BODIPY ($\phi_F = 0.80$) [11] shows that the introduction of the electron-donor *N,N*-dimethylamino-naphthyl moiety at the BODIPY *meso*-position (BODIPY **1** and **2**) leads to a dramatically decrease of the ϕ_F values. It should be noted that, in

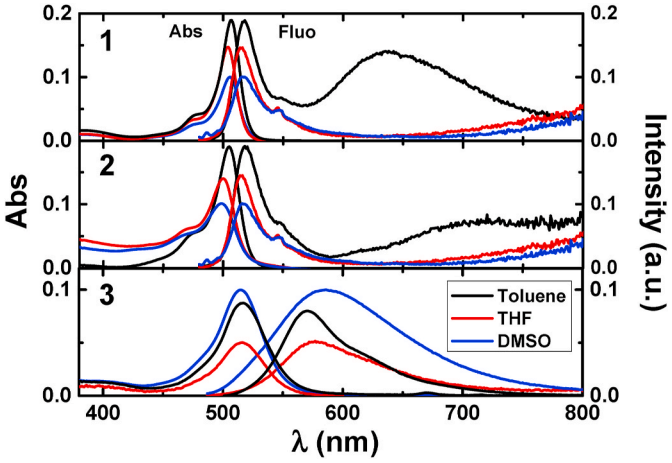

Fig. 2. Room temperature absorption and fluorescence emission spectra for the investigated BODIPY derivatives in toluene, tetrahydrofuran (THF) and dimethylsulfoxide (DMSO) solution.

Table 1
Spectroscopic (absorption, fluorescence and triplet absorption maxima) and photophysical data (including fluorescence, ϕ_F, internal conversion, ϕ_{IC}, and singlet oxygen sensitization, ϕ_Δ, quantum yields together with fluorescence lifetimes, τ_F, and triplet lifetimes, τ_T) for the BODIPY derivatives in THF solution (unless noted) at 293 K.

Compound	λ^{Abs}_{max} (nm)	λ^{Fluo}_{max} (nm)	$\lambda^{T_i \rightarrow T_n}_{max}$ [a] (nm)	ϕ_F	τ_F [a] (ns)	ϕ_Δ	τ_T (μs)
1	500	515	550	0.058[a]	3.3[c]	0.84[a]	24[a]
				0.004		0.16	85
				0.005[b]		0.04[b]	
2	495	515	550	0.047[a]	4.4[c]	0.29[a]	48[a]
				0.007		0.05	100
				0.005[b]		0.02[b]	
3	515	576	430	0.56[a]	4.2	0.10[a]	85[a]
				0.33		0.15	
				0.14[b]		0.17[b]	

[a] Data in toluene.
[b] Data in DMSO.
[c] Characteristic fluorescence lifetime value of the BODIPY local excited state.

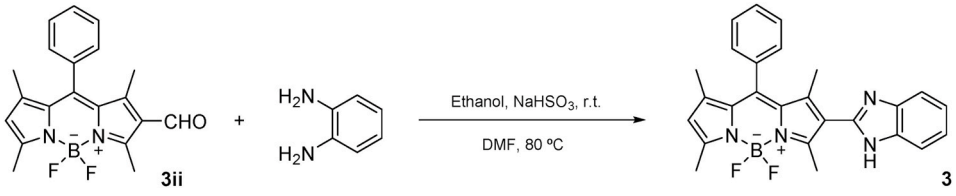

Scheme 2. Synthesis of phenyl-substituted BODIPY derivative **3**.

general, the small Stokes-shift and high ϕ_F values found for the non-substituted BODIPY are properties independent of solvent environment [33]. Therefore, the strong emission quenching found for BODIPY **1** and **2** is attributed to photoinduced electron transfer in the excited state from the BODIPY core to the aminonaphthyl *meso*-substituent. For BODIPY **3** the positive solvatokinetic effect going from non-polar to polar solvents shows that photoinduced electron transfer should occur between the BODIPY and benzimidazole groups.

To gain further insight into the molecular properties, DFT calculations for BODIPY **1**–**3** were carried out at the PBE1PBE/6-311g(d,p) level [34]. The calculated structures do not show negative frequencies, inferring that the optimized geometries are in the global energy minima. The frontier molecular orbitals in Fig. S1 in SI, show that the electron density in the HOMO orbital is spread between the aminonaphthyl or benzimidazole units and the BODIPY while the LUMO is localized in the BODIPY core. Thus, demonstrating that photoinduced electron transfer exists between BODIPY and the aminonaphthyl moieties in BODIPY **1** and **2**, and benzimidazole in BODIPY **3** [18].

The fluorescence decays for BODIPY's **1**–**3** in toluene solutions were obtained by time correlated single photon counting using as excitation source a 451 nm picoled (IRF_{FWHM}~ 90 ps) or a 460 nm nanoled (IRF_{FWHM}~ 1 ns). For BODIPY **1** and **2** the decays were collected in the characteristic emission of the locally excited state, LE, (~520 nm) and of the charge transfer band, CT, (~650 nm), see Fig. S2 in SI and Fig. 2. The global fit analysis showed that the decays are well fitted with a biexponential decay law with lifetimes (i) for BODIPY **1** of 3.3 ns associated to the decay of the LE state and a longer decay time of 6.9 ns attributed to the CT emission; (ii) for BODIPY **2** on the contrary and based on the weight of the preexponential values (a_{ij}) at the characteristic emission wavelengths of the LE and CT bands (see Fig. S2 in SI) the LE display a lifetime of 4.4 ns while a shorter value of 1.7 ns was found for the CT state.

The fluorescence decay for **3** collected at 570 nm in toluene solution was found to be well fitted with a mono-exponential decay law, displaying a fluorescence lifetime of 4.2 ns (see Fig. S2 and Table 1).

3.2. Singlet oxygen photosensitization

To evaluate the potential of the BODIPY derivatives as PDT agents, singlet oxygen sensitization quantum yields (ϕ_Δ) were obtained by direct measurement of the characteristic phosphorescence emission of $^1O_2$ at 1276 nm, after excitation at 355 nm of aerated toluene, THF and DMSO solutions of the BODIPY derivatives (see Fig. S3 in SI). The observed kinetic traces were attributed to the photosensitized phosphorescence emission decay of singlet oxygen since: (i) these were well fitted with a single-exponential decay law with lifetimes of ~29.5 μs in toluene, ~20.8 μs in THF and ~5.5 μs in DMSO solution, which are in good agreement with the characteristic lifetimes of singlet oxygen in these solvents (31.9 μs, 20.2 μs and 5.7 μs, respectively) [35–37]; and (ii) the signal was quenched when degassing the solutions with N_2 for at least 20 min.

The ϕ_Δ values were determined using a comparative method (using phenalenone as reference photosensitizer) by plotting the initial phosphorescence intensity (at 1276 nm) as a function of the laser dose and comparing the slope with that obtained for the reference compound obtained in identical experimental conditions, see Fig. 3 and Table 1. The ϕ_Δ values were corrected for the absorbance of the samples and reference compound (less than 0.3) at the laser excitation wavelength, 355 nm. Noteworthy is the remarkable enhancement of singlet oxygen sensitization efficiency for the *meso*-substituted naphthylamine BODIPY **1** and **2** going from the polar solvents (in THF solution $\phi_\Delta = 0.16$ and 0.05 while in DMSO, $\phi_\Delta = 0.04$ and 0.02, respectively) to the non-polar toluene, $\phi_\Delta = 0.84$ and 0.29, respectively). Opposite behaviour was found for the 2-substituted benzimidazole BODIPY **3** were a small increase in the ϕ_Δ values was observed going from toluene to DMSO (ϕ_Δ values ranging from 0.10 in toluene to 0.17 in DMSO, see Table 1).

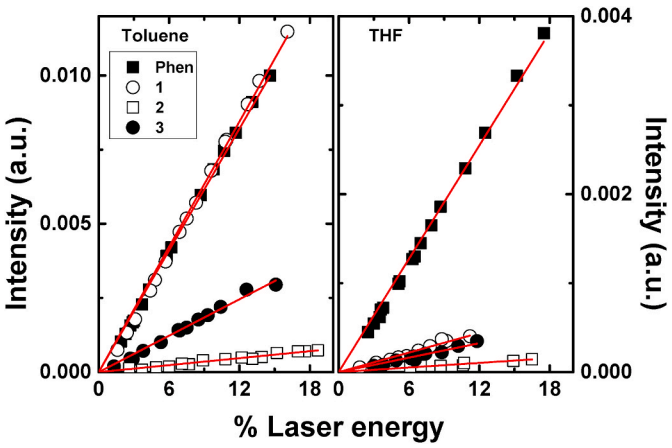

Fig. 3. Room temperature plots of the initial phosphorescence of singlet oxygen at 1276 nm as a function of laser intensity together with the best linear fits to the data points (from where the slopes for the ϕ_Δ determination were obtained) collected in air saturated solutions of the reference compound phenalenone (Phen) and the BODIPY derivatives in similar experimental conditions.

Comparison between **1** and **2** shows that the introduction of the electron-acceptor formyl group in position 2 of the BODIPY core decreases the singlet oxygen sensitization efficiency in toluene solution ($\phi_\Delta = 0.85$ *vs.* 0.29, respectively).

Similar to what was previously reported [16], for BODIPY **1** and **2** the higher singlet oxygen sensitization quantum yields together with the ICT emission bands found in toluene shows that the triplet state depends on the charge transfer state. In polar solvents, the ICT state is very weak thus the triplet state is not efficiently populated, which explains the observed lower singlet oxygen quantum yields (Table 1). These results may be explained qualitatively by the effects of solvent polarity on the energetic ordering of the LE and CT states of **1** and **2** [27]. In polar solvents, the CT state has a higher energy than the LE state, therefore, intersystem crossing to the triplet manifold is not favored, and internal conversion is dominant, as demonstrated in Table 1 by the low ϕ_F values of BODIPY **1** and **2**; ii) in nonpolar solvents, the CT states are stabilized relative to the ground state, and the CT state lies below the LE state and the intramolecular charge transfer becomes favorable prompting intersystem crossing.

3.3. Pump-probe transient absorption spectroscopy

To further investigate the excited state dynamics of the investigated BODIPY derivatives the time-resolved femtosecond and the nanosecond transient difference absorption spectra were obtained in toluene solution (where singlet oxygen generation is favored through efficient triplet state energy transfer).

The femtosecond transient absorption (fs-TA) was collected in the wavelength range from 340 nm to 750 nm in a 7.6 ns time window, see Fig. 4. The samples were excited in the lowest energy $S_1 \leftarrow S_0$ absorption band, at 515 nm (BODIPY **1** and **2**) and 540 nm (BODIPY **3**), using low laser pump energies (≤300 nJ) to avoid nonlinear effects. In general, the TA spectra of aerated toluene solutions of the investigated polymers are composed of a broad positive excited state absorption (ESA) in the 350–470 nm and 540–700 nm range, and negative strongly overlapped bands resulting from bleaching of the ground state absorption, GSA, (centred at ~510 nm for BODIPY **1** and **2**, and ~525 nm for **3**) and stimulated emission (>520 nm, **1** and **2**, and >560 nm, **3**), see Figs. 4 and 2.

As shown in Fig. 4, in general, in the first 2 ns the initially formed ESA band (which is attributed to the S_1–S_n ESA) gradually red shifts and thereon the band maxima remain unchanged (not decaying completely) up to the longest delay time measured. Based on the long-lived nature of

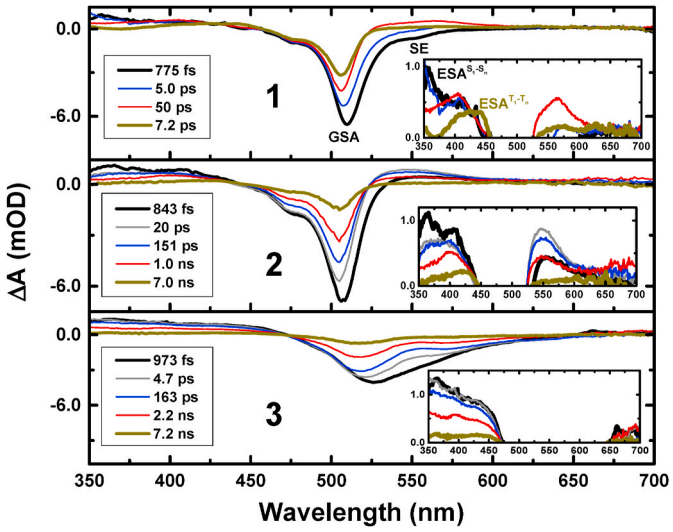

Fig. 4. Room temperature time resolved transient absorption spectra for the investigated BODIPY derivatives in aerated toluene solutions after 250 fs laser pulse (IRF) at excitation wavelength of 515 nm (**1** and **2**) and 540 nm (**3**). As inset is highlighted the positive excited state absorption band (ESA) that results from the contribution of ESA^{S1-Sn} at shorter delays and ESA^{T1-Tn} at longer delay times.

the latter band and the good agreement between the spectroscopic data obtained in the fs-TA at longer delay times and the triplet absorption bands obtained by ns-TA (see Fig. S2 in SI) this spectroscopic feature is attributed to the T_1-T_n ESA.

The triplet-triplet transient absorption spectra of deaerated solutions of the BODIPY derivatives were collected by nanosecond-millisecond pump-probe transient absorption spectroscopy (Fig. S4 in SI). Similar transient triplet-triplet absorption spectra and triplet lifetimes (τ_T = 24–100 μs) were found in toluene and THF solution (Table 1). The triplet nature of the transient absorption signals is supported by their quenching by oxygen in air-saturated solutions which follows pseudo first order kinetics.

3.4. Kinetic analysis

Global fit analysis (using the principal component analysis methodology) was performed after singular value decomposition to better describe the observed ultrafast TAS dynamics. The analysis was performed using all the kinetics in the 360–725 nm range and taking into account the transient lifetimes obtained in the ns-TA data (*i.e.*, fixing the long decay time in the analysis to the triplet lifetime). In general, the transient decays were well fitted with the sum of four exponentials, see Fig. S5 in SI and Table 2. Therefore, the excited state dynamics of the investigated BODIPY can be described with a series of sequential steps, see Scheme 3. In agreement with previous works [33,38–40], we propose that after light absorption to the excited Franck-Condon state (FC); (i) fast FC relaxation and solvent-related reorganization occurs to form the locally excited state (transient lifetime values ranging from 0.44 ps to 4 ps, τ_1); (ii) from here charge separation concomitantly with conformational evolution (associated with BODIPY-core structural changes in the excited state) give rise to the charge transfer state (CT) discussed above (τ_2 in the 50–87 ps range). Indeed, although the methyl groups at the 1,3,5-positions hinder the rotation of the substituent groups at the *meso*- and β-positions, it was shown that bending of the BODIPY-core occurs in the excited state [38]. Finally the CT state can deactivate to the ground state or lead to triplet-state formation (through charge recombination) [41] with transient lifetimes in the 1.5–3.8 ns range (that are in agreement with the fluorescence lifetimes obtained by single photon counting, Table 1).

Table 2
Transient decay lifetimes (τi) obtained from the global fit analysis to the TAS data (i.e., simultaneous analysis of the decays collected in the 360–725 nm range) for the investigated BODIPY derivatives in toluene solution.

Compound	τ_1 (ps)	τ_2 (ps)	τ_3 (ns)	τ_4 (μs)[a]
1	4	50	2.9	24
2	0.44	44	1.5	48
3	1.7	87	3.8	85

[a] Fixed in the analysis to the triplet lifetime.

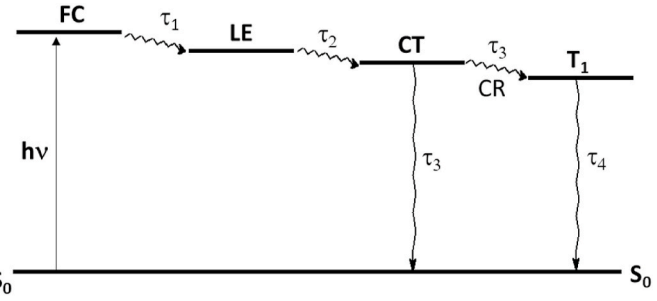

Scheme 3. Representation of the excited state dynamics of the investigated BODIPY derivatives in toluene, where FC represents the Frank-Condon state, LE – locally excited state, CT-charge transfer state, CR – charge recombination and T_1-triplet excited state.

4. Conclusion

In conclusion, three aryl-BODIPY derivatives with electron-donor and electron withdrawing groups at *meso* and 2-position, respectively, were synthesized and the effects of the substituent groups and solvent polarity on the singlet oxygen generation efficiency was investigated. It was seen that electron-donating groups at the *meso*-position strongly enhances singlet oxygen photosensitization in non-polar solvents while the introduction of a benzimidazole electron-deficient heterocycle at position 2 of the BODIPY core does not significantly enhance singlet oxygen generation. Triplet state formation was found to be mediated by the occurrence of a charge separated state in the investigated BODIPY derivatives.

CRediT author contribution statement

Raquel C.R. Gonçalves: performed the synthetic work, Formal analysis. **João Pina:** carried out the spectroscopic and photophysical characterization, the theoretical calculations, Writing – original draft. **Susana P.G. Costa:** Methodology, Supervision. **M. Manuela M. Raposo:** Methodology, Supervision, Writing – original draft.

Declaration of competing interest

The authors declare that they have no known competing financial interests or personal relationships that could have appeared to influence the work reported in this paper.

Acknowledgments

This work was supported by the Fundaçaõ para a Ciência e a Tecnologia (FCT), Portuguese Agency for Scientific Research, through the Coimbra Chemistry Centre projects UIDB/00313/2020 and UIDP/00313/2020 and through the Centro de Química (CQUM), project UID/QUI/00686/2020. The NMR spectrometer Bruker Avance III 400 is part of the National NMR Network and was purchased within the framework of the National Program for Scientific Reequipment, contract REDE/1517/RMN/2005 with funds from POCI 2010 (FEDER) and FCT.

Raquel C. R. Gonçalves acknowledges FCT for funding (SFRH/BD/05278/2020). The research leading to these results has received funding from Laserlab-Europe (grant agreement no. 284464, EC's Seventh Framework Programme).

Appendix A. Supplementary data

Supplementary data to this article can be found online at https://doi.org/10.1016/j.dyepig.2021.109784.

References

[1] Ghosh N, Das A, Chaffee S, Roy S, Sen CK. Chapter 4 - reactive oxygen species, oxidative damage and cell death. In: Chatterjee S, Jungraithmayr W, Bagchi D, editors. Immunity and inflammation in health and disease. Academic Press; 2018. p. 45–55.
[2] Kwiatkowski S, Knap B, Przystupski D, Saczko J, Kędzierska E, Knap-Czop K, Kotlińska J, Michel O, Kotowski K, Kulbacka J. Photodynamic therapy – mechanisms, photosensitizers and combinations. Biomed Pharmacother 2018;106:1098–107.
[3] Castano AP, Demidova TN, Hamblin MR. Mechanisms in photodynamic therapy: part one—photosensitizers, photochemistry and cellular localization. Photodiagnosis Photodyn Ther 2004;1:279–93.
[4] Lan M, Zhao S, Liu W, Lee C-S, Zhang W, Wang P. Photosensitizers for photodynamic therapy. Adv. Healthc. Mater. 2019;8:1900132.
[5] Jiang Z, Shao J, Yang T, Wang J, Jia L. Pharmaceutical development, composition and quantitative analysis of phthalocyanine as the photosensitizer for cancer photodynamic therapy. J Pharmaceut Biomed Anal 2014;87:98–104.
[6] Dąbrowski JM, Pucelik B, Regiel-Futyra A, Brindell M, Mazuryk O, Kyzioł A, Stochel G, Macyk W, Arnaut LG. Engineering of relevant photodynamic processes through structural modifications of metallotetrapyrrolic photosensitizers. Coord Chem Rev 2016;325:67–101.
[7] Abrahamse H, Hamblin MR. New photosensitizers for photodynamic therapy. Biochem J 2016;473:347–64.
[8] Kamkaew A, Lim SH, Lee HB, Kiew LV, Chung LY, Burgess K. BODIPY dyes in photodynamic therapy. Chem Soc Rev 2013;42:77–88.
[9] Kue CS, Ng SY, Voon SH, Kamkaew A, Chung LY, Kiew LV, Lee HB. Recent strategies to improve boron dipyrromethene (BODIPY) for photodynamic cancer therapy: an updated review. Photochem Photobiol Sci 2018;17:1691–708.
[10] Awuah SG, You Y. Boron dipyrromethene (BODIPY)-based photosensitizers for photodynamic therapy. RSC Adv 2012;2:11169–83.
[11] Loudet A, Burgess K. BODIPY dyes and their Derivatives: syntheses and spectroscopic properties. Chem Rev 2007;107:4891–932.
[12] Collado D, Casado J, González SR, Navarrete JTL, Suau R, Perez-Inestrosa E, Pappenfus TM, Raposo MMM. Enhanced functionality for donor–acceptor oligothiophenes by means of inclusion of BODIPY: synthesis, electrochemistry, Photophysics, and model Chemistry. Chem Eur J 2011;17:498–507.
[13] Lo Presti M, Martínez-Máñez R, Ros-Lis JV, Batista RMF, Costa SPG, Raposo M, M M, Sancenón F. A dual channel sulphur-containing a macrocycle functionalised BODIPY probe for the detection of Hg(ii) in a mixed aqueous solution. New J Chem 2018;42:7863–8.
[14] Niu SL, Massif C, Ulrich G, Ziessel R, Renard P-Y, Romieu A. Water-solubilisation and bio-conjugation of a red-emitting BODIPY marker. Org Biomol Chem 2011;9:66–9.
[15] Orte A, Debroye E, Ruedas-Rama MJ, Garcia-Fernandez E, Robinson D, Crovetto L, Talavera EM, Alvarez-Pez JM, Leen V, Verbelen B, Cunha Dias de Rezende L, Dehaen W, Hofkens J, Van der Auweraer M, Boens N. Effect of the substitution position (2, 3 or 8) on the spectroscopic and photophysical properties of BODIPY dyes with a phenyl, styryl or phenylethynyl group. RSC Adv 2016;6:102899–913.
[16] Hu W, Zhang X-F, Lu X, Lan S, Tian D, Li T, Wang L, Zhao S, Feng M, Zhang J. Attaching electron donating groups on the meso-phenyl and meso-naphthyl make aryl substituted BODIPYs act as good photosensitizer for singlet oxygen formation. J Lumin 2018;194:185–92.
[17] Chen K, Dong Y, Zhao X, Imran M, Tang G, Zhao J, Liu Q. Bodipy derivatives as triplet photosensitizers and the related intersystem crossing mechanisms. Front. Chem. 2019;7.
[18] Li Z, Li L-J, Sun T, Liu L, Xie Z. Benzimidazole-BODIPY as optical and fluorometric pH sensor. Dyes Pigments 2016;128:165–9.
[19] Epelde-Elezcano N, Martínez-Martínez V, Peña-Cabrera E, Gómez-Durán CFA, Arbeloa IL, Lacombe S. Modulation of singlet oxygen generation in halogenated BODIPY dyes by substitution at their meso position: towards a solvent-independent standard in the vis region. RSC Adv 2016;6:41991–8.
[20] Jiao L, Yu C, Li J, Wang Z, Wu M, Hao E. β-Formyl-BODIPYs from the Vilsmeier–Haack reaction. J Org Chem 2009;74:7525–8.
[21] Montalti M, Credi A, Prodi L, Gandolfi M. Handbook of photochemistry. Boca Raton: CRC Press; 2006.
[22] Seixas de Melo J, Pina J, Dias FB, Maçanita AL. In: Photochemistr Applied, Evans R, Douglas P, Burrows HD, editors. Experimental techniques for excited state characterisation. Dordrecht: Springer; 2013. p. 533–85.
[23] Striker G, Subramaniam V, Seidel CAM, Volkmer A. Photochromicity and fluorescence lifetimes of green fluorescent protein. J Phys Chem B 1999;103:8612–7.
[24] Frisch MJ, Trucks GW, Schlegel HB, Scuseria GE, Robb MA, Cheeseman JR, Scalmani G, Barone V, Mennucci B, Petersson GA, Nakatsuji H, Caricato M, Li X, Hratchian HP, Izmaylov AF, Bloino J, Zheng G, Sonnenberg JL, Hada M, Ehara M, Toyota K, Fukuda R, Hasegawa J, Ishida M, Nakajima T, Honda Y, Kitao O, Nakai H, Vreven T, Montgomery Jr JA, Peralta JE, Ogliaro F, Bearpark M, Heyd JJ, Brothers E, Kudin KN, Staroverov VN, Kobayashi R, Normand J, Raghavachari K, Rendell A, Burant JC, Iyengar SS, Tomasi J, Cossi M, Rega N, Millam JM, Klene M, Knox JE, Cross JB, Bakken V, Adamo C, Jaramillo J, Gomperts R, Stratmann RE, Yazyev O, Austin AJ, Cammi R, Pomelli C, Ochterski JW, Martin RL, Morokuma K, Zakrzewski VG, Voth GA, Salvador P, Dannenberg JJ, Dapprich S, Daniels AD, Farkas O, Foresman JB, Ortiz JV, Cioslowski J, Fox DJ. Gaussian 09, revision A.02. Wallingford CT: Gaussian, Inc.; 2009.
[25] Adamo C, Barone V. Toward reliable density functional methods without adjustable parameters: the PBE0 model. J Chem Phys 1999;110:6158–70.
[26] Pina J, Queiroz MJRP, Seixas de Melo J. Effect of substitution on the ultrafast deactivation of the excited state of benzo[b]thiophene-arylamines. Photochem Photobiol Sci 2016;15:1029–38.
[27] Flors C, Nonell S. On the phosphorescence of 1H-Phenalen-1-one. Helv Chim Acta 2001;84:2533–9.
[28] Redmond RW, Gamlin JN. A compilation of singlet oxygen yields from biologically relevant molecules. Photochem Photobiol 1999;70:391–475.
[29] Schmidt R, Tanielian C, Dunsbach R, Wolff C. Phenalenone, a universal reference compound for the determination of quantum yields of singlet oxygen O2(1Δg) sensitization. J Photochem Photobiol Chem 1994;79:11–7.
[30] Wilkinson F, Helman WP, Ross AB. Quantum yields for the photosensitized formation of the lowest electronically excited singlet state of molecular oxygen in solution. J Phys Chem Ref Data 1993;22:113–262.
[31] Godard J, Brégier F, Arnoux P, Myrzakhmetov B, Champavier Y, Frochot C, Sol V. New phenalenone derivatives: synthesis and evaluation of their singlet oxygen quantum yield. ACS Omega 2020;5:28264–72.
[32] Wagner RW, Lindsey JS. Boron-dipyrromethene dyes for incorporation in synthetic multi-pigment light-harvesting arrays. Pure Appl Chem 1996;68:1373–80.
[33] Kim S-Y, Cho Y-J, Son H-J, Cho DW, Kang SO. Photoinduced electron transfer in a BODIPY-ortho-carborane dyad investigated by time-resolved transient absorption spectroscopy. J Phys Chem 2018;122:3391–7.
[34] Laine M, Barbosa NA, Wieczorek R, Melnikov MY, Filarowski A. Calculations of BODIPY dyes in the ground and excited states using the M06-2X and PBE0 functionals. J Mol Model 2016;22:260.
[35] Okiyasu S, Jun W, Keiichi I, Shizuo N. Absolute quantum yields and lifetimes of photosensitized phosphorescence of singlet oxygen O2 (1Δg) in air-saturated aqueous and organic solutions of phenalenone. Chem Lett 1999;28:67–8.
[36] Nilsson R, Kearns DR. Role of singlet oxygen in some chemiluminescence and enzyme oxidation reactions. J Phys Chem 1974;78:1681–3.
[37] Yu C, Canteenwala T, El-Khouly ME, Araki Y, Pritzker K, Ito O, Wilson BC, Chiang LY. Efficiency of singlet oxygen production from self-assembled nanospheres of molecular micelle-like photosensitizers FC4S. J Mater Chem 2005;15:1857–64.
[38] Suhina T, Amirjalayer S, Woutersen S, Bonn D, Brouwer AM. Ultrafast dynamics and solvent-dependent deactivation kinetics of BODIPY molecular rotors. Phys Chem Chem Phys 2017;19:19998–20007.
[39] Tarafdar G, Johnson JC, Larson BW, Ramamurthy PC. BODIPY based A-D-A molecules: effect of CF3 group substitution at meso phenyl group. Dyes Pigments 2020;177:108289.
[40] Scholz M, Hoffmann C, Klein JR, Wirtz M, Jung G, Oum K. Exploring differences in excited-state properties of styryl-BODIPY chromophores upon change from α- to β-substitution. Z Phys Chem 2019:20191374.
[41] Bandi V, Gobeze HB, Lakshmi V, Ravikanth M, D'Souza F. Vectorial charge separation and selective triplet-state formation during charge recombination in a pyrrolyl-bridged BODIPY–fullerene dyad. J Phys Chem C 2015;119:8095–102.